Catalysis Today 144 (2009) 177–182

Contents lists available at ScienceDirect

Catalysis Today

journal homepage: www.elsevier.com/locate/cattod

Oxygen vacancies and OH species in rutile and anatase TiO_2 polymorphs

Aldo Amore Bonapasta [a,*], Francesco Filippone [a], Giuseppe Mattioli [a,b], Paola Alippi [a]

[a] Istituto di Struttura della Materia, Consiglio Nazionale delle Ricerche, Via Salaria km 29.5, CP 10, 00016 Monterotondo Stazione, Roma, Italy
[b] Universita degli Studi di Roma "La Sapienza", Piazzale Aldo Moro 5, 00185 Roma, Italy

ARTICLE INFO

Article history:
Available online 9 March 2009

Keywords:
Defects
Density functional theory
Titanium dioxide

ABSTRACT

Ab initio density functional calculations in the beyond-LSD (Local Spin Density), LSD + U approximation have been performed to investigate the properties of bridging hydroxyls (OHb) at the rutile (1 1 0) and anatase (1 0 1) surfaces as well as of bulk oxygen vacancies (VOx) and Ti–OH defects in the same two polymorphs. The aim of this study is to deepen our understanding of the properties of these defects both in rutile and anatase as well as to reveal similar behaviours of VOx and OH defects. In the case of rutile OHbs, a good agreement is found between present results and those of a recent STM study. Anatase OHbs show properties similar to those of rutile OHbs. On the contrary, a remarkable difference is found between the structural and electronic properties of bulk VOxs in rutile and anatase, which could explain the higher electron mobility and photocatalytic activity observed for the latter compound. Bulk Ti–OH defects are predicted to easily form through insertion of atomic H in TiO_2 lattices. Moreover, in the case of rutile, these defects should present properties quite similar to those of VOxs. Finally, the results achieved here stress the importance of beyond-LSD methods when dealing with defects in TiO_2.

1. Introduction

Titanium dioxide is one of the most important and most widely used metal oxides for technological applications including, e.g., photocatalysis, production of hydrogen and electric energy in solar cells, and use in spintronic devices after doping with magnetic impurities [1–3]. Oxygen vacancies (VOx) and OH surface species can significantly affect the properties of TiO_2. For instance, photocatalysis begins by creating an electron (e) in the conduction band and a hole (h) in the valence band by optical excitation. These excited carriers diffuse to the surface to initiate chemical reactions with adsorbed molecules, while e–h recombination, possibly favoured by impurities or defects, represents a competing process which tends to prevent the carriers for reaching the surface. Thus, the efficiency of a photocatalytic process is affected by: (i) the region of absorption of electromagnetic radiation, possibly extended from UV (the region of undoped, stoichiometric TiO_2) to visible and IR regions, (ii) the absorption rate of the semiconductor, which influences the initial number of photo-excited carriers, and (iii) the time required for the carriers to move to the surface to initiate reactions, as compared to their recombination lifetime. Clearly, electronic levels induced by defects, like VOx, in the TiO_2 energy gap can influence the TiO_2 properties, e.g., shallow levels can significantly increase the electron conductivity while deep levels can permit optical excitation in the visible or IR regions. Oxygen vacancies form in appreciable concentrations in the bulk and at the surface of TiO_2 nanoparticles, polycrystal or single crystal samples whose preparation techniques include heavy heating treatments causing a broad chemical reduction of these materials. These defects behave as donors, thus possibly accounting for the usual *n*-type behaviour of TiO_2 samples [1,2,4,5]. Generally, such an effect is induced by bulk VOxs. In fact, water dissociation occurs at surface VOx sites, both on anatase [6], and rutile surfaces [7], leading to the formation of two bridging hydroxyl groups (2OHb), see Fig. 1(A), for every VOx. Such a filling mechanism is a very efficient one: it has been recently reported that, even in deep ultra high vacuum (UHV) conditions, VOxs are hardly observed on the rutile (1 1 0) surface because even a little amount of residual water molecules very quickly converts a reduced surface into an hydroxylated one [8,9]. Thus, OHbs basically replace VOxs at TiO_2 surfaces. Regarding the relationships existing between surface VOxs and surface bridge OH groups, some recent experimental and theoretical studies deserve a particular consideration. A theoretical study has shown that OHb and VOx defects at the rutile (1 1 0) surface induce quite similar, deep electronic states in the energy gap, suggested that such surface defects can affect the recombination time by trapping the excited carriers, and stressed the importance of beyond-LSD (Local Spin Density) methods, e.g., the use of hybrid functionals, when dealing with such defects [10]. A combined theoretical and STM (scanning tunnelling microscopy) study of the same surface has given details on the properties of 2OHb pairs and isolated OHbs

* Corresponding author.
E-mail address: aldo.amore@ism.cnr.it (A. Amore Bonapasta).

0920-5861/$ – see front matter © 2009 Elsevier B.V. All rights reserved.
doi:10.1016/j.cattod.2009.01.047

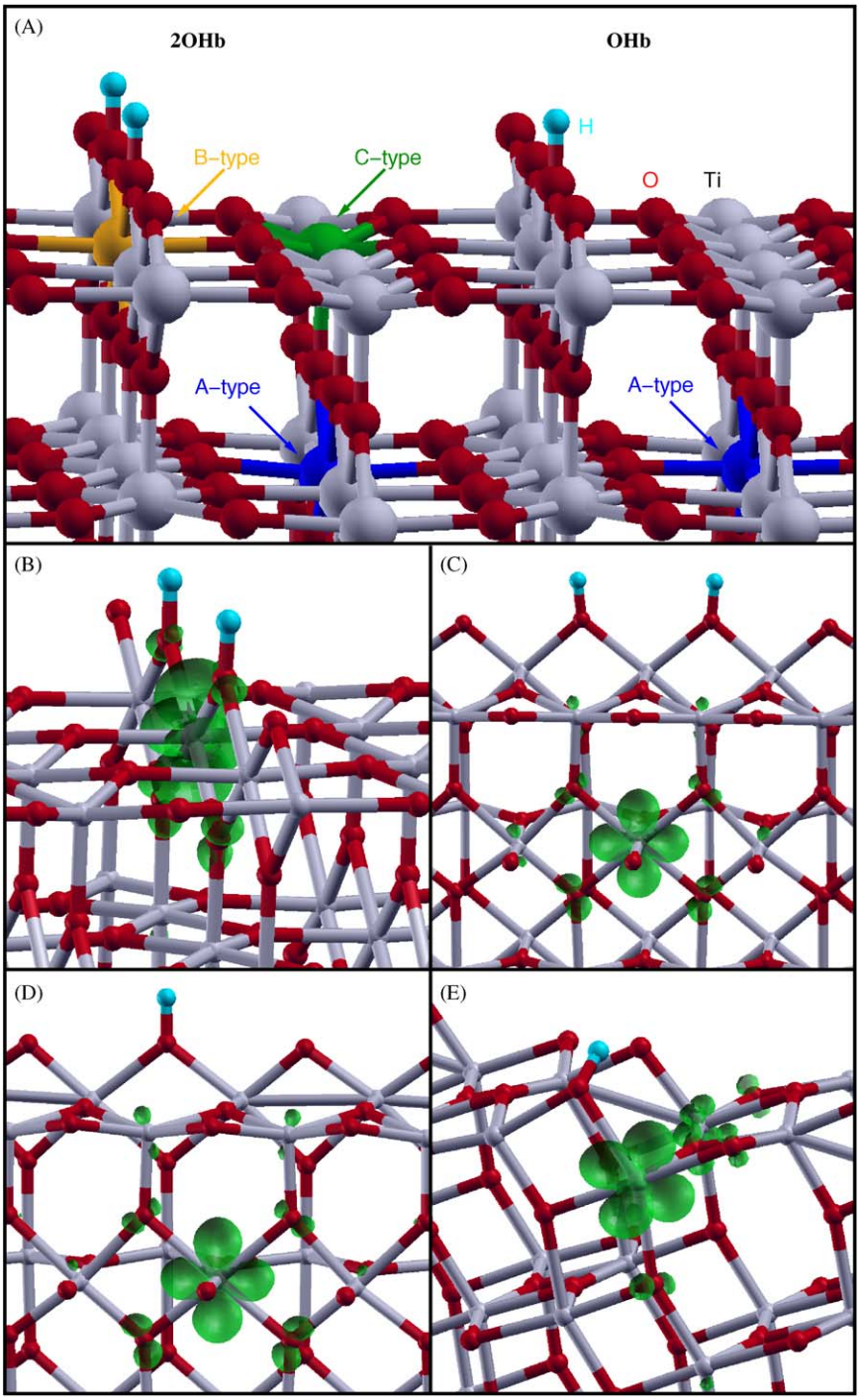

Fig. 1. (A) Relaxed geometries of the rutile (1 1 0) surface (side view) with coupled (2OHb) and isolated bridging hydroxyl (OHb) defects. "A-type", "B-type", and "C-type" labels indicate possible sites of reduced Ti^{3+} atoms induced by OHb defects. (B)–(D) Local geometry of 2OHb and isolated OHb defects and spin density plots showing the charge localization of the corresponding electronic levels: (B) 2OHb at the rutile (1 1 0) surface with the charge of a first electronic level localized at a surface B-type Ti^{3+} atom; (C) the same defect with the charge of a second electronic level localized at a subsurface A-type Ti^{3+} atom; (D) isolated OHb at the same rutile surface with charge localized at a subsurface A-type Ti^{3+} atom; (E) isolated OHb at the anatase (1 0 1) surface with charge localized at a surface Ti^{3+} atom.

at the same surface [8,11]. Inspired by these recent studies, here, we present an extensive, theoretical investigation of the properties of VOxs and OH-related defects. Our aim is to deepen the understanding of the properties of these defects both in rutile and anatase, as well as to reveal similar behaviours of VOx and OH defects in either TiO_2 polymorphs. This work has been developed along three lines. First, deep investigation of the OHb properties at the rutile (1 1 0) surface and comparison with the recent STM results mentioned above, as well as extension of the investigation to the properties of the same defect at the (1 0 1) anatase surface. We have also checked the reliability of our beyond-LSD, LSD + U [12] theoretical approach by comparing our results with those achieved using hybrid functionals [10]. Second, study of the VOx's properties in the *bulk* of rutile and anatase. Third, investigation of bulk Ti–OH complexes formed by atomic H inserted in the TiO_2 lattice. In this regard, previous studies have investigated different effects of H in rutile like, e.g., H charge-balancing of impurities [13] or effects of H intercalation [14]. On the other hand, although Ti–

OH defects could affect the TiO_2 electronic properties by inducing defect states in the energy gap, there is scarce information on the properties of such defects, in particular on their electronic properties, both in rutile and anatase. We have focussed therefore on the stability and electronic properties of isolated Ti–OH in both TiO_2 polymorphs and performed a comparison with the electronic properties of bulk VOxs.

The results of our study provide novel, complementary information on the VOx and OHb defects in anatase and rutile as well as on their effects on the properties of the two TiO_2 polymorphs. They can be summarized as in the following. Our results agree with those achieved by using hybrid functionals [10] and with the mentioned STM findings in the case of OHbs at the rutile (1 1 0) surface [8,11]. They also predict small differences between these defects and OHbs at the anatase (1 0 1) surface. In the case of bulk VOxs, we report instead a marked difference between the electronic properties of such defects in rutile and anatase: in the former compound, VOxs induce only two deep levels in the energy gap, while in the latter they induce one deep and one *shallow* level. This is a remarkable result which can account for some differences between the properties of these two TiO_2 polymorphs important for the technological applications, like the higher photocatalytic activity and electron mobility of anatase with respect to rutile [1,2,15,16]. Finally, present results indicate that bulk Ti–OH defects are quite stable and easily form in both polymorphs. In rutile, these defects present properties quite similar to those of bulk VOxs. This suggests that possible, beneficial effects of the VOxs on the material properties, like the occurrence of optical absorption in the visible region, could be also achieved through a mild hydrogenation.

2. Methods

Defects in anatase and rutile have been investigated by using DFT methods as developed in the Quantum-ESPRESSO package [17]. Total energy calculations have been performed inside a (beyond-LSD) LSD + U approach [12,18]. Total energies have been calculated in a supercell approach, by using ultrasoft pseudopotentials [19] and the PBE gradient corrected exchange-correlation functional [20]. Satisfactorily converged results have been achieved by expanding Kohn-Sham orbitals in plane waves up to energy cutoffs of 25 and 150 Ry for the wavefunctions and the charge density, respectively. A self-consistent Hubbard U correction of 3.4 eV (3.3 eV) for the *d* electrons of rutile (anatase) Ti atoms has been calculated by using the linear response approach described in Ref. [18]. $2 \times 2 \times 4$ 96-atoms and $3 \times 3 \times 1$ 108-atoms supercells have been used to simulate bulk rutile and anatase, respectively, together with a $2 \times 2 \times 2$ Monkhorst-Pack **k**-point mesh. A 96-atoms c(4×2) surface cell, formed by adding about 12 Å of vacuum space to four O–Ti–O atomic layers, with a $2 \times 2 \times 1$ **k**-point Monkhorst-Pack mesh has been used for the rutile (1 1 0) surface. A 96-atoms 2×1 surface cell, formed by adding about 12 Å of vacuum space to four O–Ti–O atomic layers, with a $2 \times 2 \times 1$ **k**-point Monkhorst-Pack mesh has been used for the anatase (1 0 1) surface. Both these configurations correspond to one OHb defect every four bridging oxygen atoms.

Geometry optimization procedures have been performed by minimizing the atomic forces of all of the atoms in the bulk supercells and of the atoms of the first and second topmost layers of the surface supercells. In the latter cells, the third layer atoms have been kept fixed in their bulk positions, and the bottom layer atoms have been relaxed in a surface-like configuration. The U correction has been applied to circumvent the too poor LSD-GGA electron correlation description [10,21]. Such a correction has been checked by comparing our results with those achieved by using hybrid functionals in the cases of bulk VOx [21] and OHb and VOx [10] at the (1 1 0) surface of rutile. Electronic properties have been investigated by analyzing the Kohn-Sham eigenvalues at the Γ point, spin density of states (not reported here), and spin density distributions corresponding to the defects states.

3. Results and discussion

In this section, we will discuss the results achieved by using the LSD + U method in the investigation of the above mentioned defects. It is worth noticing that, at variance with such results, those achieved by using the LSD methods indicate that the same defects always induce quite shallow electronic levels close to the conduction band and characterized by a wide delocalization of the corresponding electronic charge on several Ti atoms, which do not agree with experimental findings, see, e.g., Refs. [22–24].

3.1. Bridging hydroxyl groups (OHb)

In the case of the rutile (1 1 0) surface, when a water molecule dissociates at a VOx site by forming a 2OHb pair [7], the two H atoms tend to lose their electrons. The results achieved by using hybrid functionals indicate that these electrons occupy two different electronic levels at 1.2 and 1.6 eV below the conduction band (CB) in a triplet state and are strongly localized on the two Ti^{3+} atoms at the surface B- and C-type sites of Fig. 1(A) [10]. Even our results find two deep donor levels localized on Ti atoms. However, there are some differences between our results and those reported in Ref. [10]. First, the electronic structure of the coupled OHb groups, characterized here by two almost degenerate electronic levels located slightly above midgap, see Fig. 2(C), seems in a better agreement with the defect level observed at 0.7–0.9 eV below the CB [22–24]. Second, at variance with the above mentioned study, the two 2OHb electrons are located at the surface B site and at the subsurface A site of Fig. 1(A), see Fig. 1(B) and (C), respectively. It may be worth noticing that the A site involves a fully coordinated Ti atom (i.e., surrounded by six O atoms) while the C site proposed in Ref. [10] corresponds to a five-fold coordinated Ti atom.

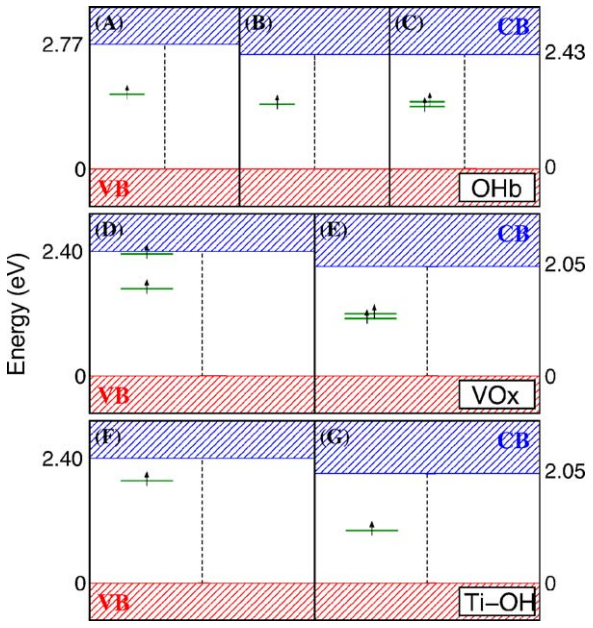

Fig. 2. Diagram of the electronic levels induced by different defects in the anatase and rutile energy gap. (A) OHb in anatase, (B) OHb in rutile, (C) 2OHb pair in rutile, (D) VOx in anatase, (E) VOx in rutile, (F) Ti–OH in anatase, and (G) Ti–OH in rutile. VB (CB) indicates the valence band maximum (conduction band minimum) as given by Kohn-Sham electronic eigenvalues.

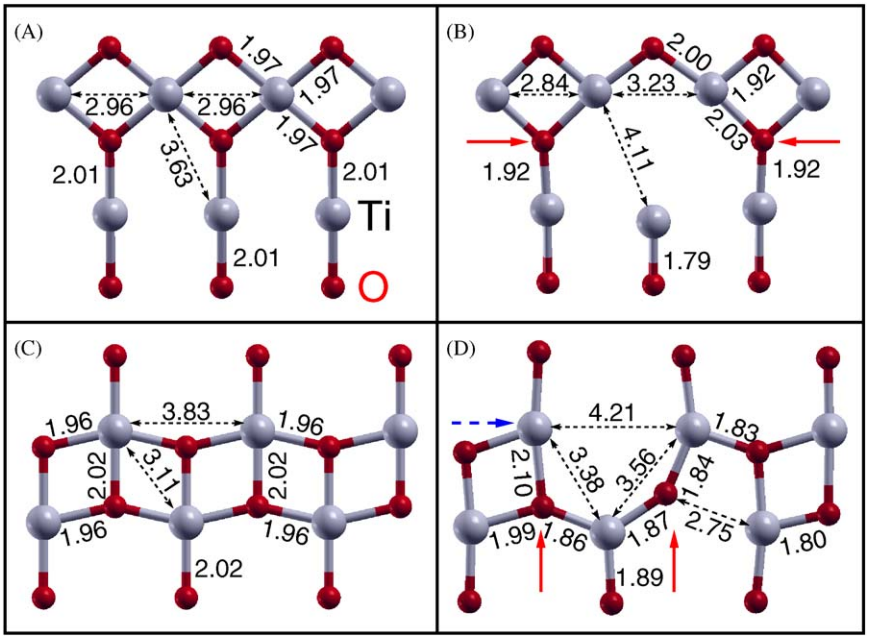

Fig. 3. Optimized geometries of bulk rutile and of an oxygen vacancy in a (1 1 0) plane are given in (A) and (B), respectively. The analogue for a (1 0 0) plane of anatase is shown in (C) and (D), respectively. The red arrows (full lines) indicate O atoms neighbouring the vacancy site (see the text). The blue arrow (dashed line) indicates the Ti atom where a charge localization occurs, see Fig. 4(C). (For interpretation of the references to color in this figure legend, the reader is referred to the web version of the article.)

Then, we have considered the separation of a 2OHb pair in two isolated OHbs. The isolated OHbs result to be more stable by 0.4 eV than a 2OHb pair, which agrees with an evolution of this defect observed by STM measurements [11]. Regarding the properties of an isolated OHb defect, the results found here for the 2OHb defect pose a question about which of the two possible localizations of the defect charge found for the 2OHb pair, surface or subsurface, should characterize an isolated OHb group. In this regard, we find that an isolated OHb induces a deep electronic level into the band gap, see Fig. 2(B), which localizes charge at a 3*d* orbital of a subsurface Ti^{3+} A-type site, see Fig. 1(D). This suggests that, in the 2OHb defect, the electronic level localized at the B-type site (see Fig. 1(B)) is related to the OHb–OHb interaction and disappears when the two OHbs are separated.

In the case of anatase, we have investigated the properties of an isolated OHb at the (1 0 1) surface. This defect induces an electronic level in the energy gap at about 1 eV from the valence band maximum (VBM), see Fig. 2(A), in agreement with experimental findings [25]. The corresponding electronic charge is localized at a *d* orbital of a surface Ti^{3+} atom, see Fig. 1(E). Thus, the properties of anatase OHbs should closely parallel those of a rutile OHbs. In particular, even in anatase an OHb defect is expected to behave as an electron trap. A small difference regards instead the localization of the defect electron, which involves a six-fold coordinated Ti atom located at a subsurface site in the case of rutile and at a surface site in anatase.

3.2. Bulk VOxs in rutile and anatase

The results achieved for bulk VOx will be presented in a synthetic form here and discussed in detail elsewhere [26]. As anticipated above, such results indicate that the electronic structure of a VOx in bulk rutile is strongly different from that of a VOx in anatase. Such a difference originates from a different local symmetry of the defect site in the two compounds which leads to quite different structural rearrangements when the O atom is removed. In turn, these different rearrangements induce quite different electronic properties. In detail, in the case of rutile, the positions of Ti and O atoms located on a (1 1 0) plane of the bulk material are shown in Fig. 3(A). The relaxed positions of the same atoms after removal of an O atom are shown in Fig. 3(B). The Ti atoms nearest neighbouring (NN) the vacancy displace within the (1 1 0) plane by moving away from the vacancy site with a sort of breathing relaxation which does not alter the local symmetry around the site of the removed O atom. A quite different picture is found for a VOx in bulk anatase. Fig. 3(C) and (D) shows Ti and O atoms located on a (1 0 0) plane of this material and their rearrangement after the vacancy formation, respectively. These figures show that, at variance with the case of rutile, the removal of an O atom induces significant changes of the local geometry around the vacancy site: an O atom neighbouring the vacancy breaks indeed its bond with a Ti atom and approaches two NN Ti atoms by strengthening the corresponding Ti–O bonds and becoming two-fold coordinated (O2c). Such different structural rearrangements are related to the existence, in anatase, of a pair of symmetrically equivalent O atoms neighbouring the vacancy (NN O) each one bonded to two NN Ti, see the red arrows (full lines) in Fig. 3(D), in contrast with rutile, where the corresponding, equivalent NN O are bonded to one NN Ti only, see the red arrows (full lines) in Fig. 3(B). In fact, an analysis of the geometry relaxation patterns shows that while in both compounds an increase of the Ti–Ti distances around the vacancy site accompanies the creation of the defect itself, only in anatase these Ti displacements favour, first, a significant displacement of the NN O atoms towards the vacancy site, then, a spontaneous evolution towards the final configuration where one of these two atoms has broken an O–Ti bond. It should be noted that: (i) differences in the atomic displacements sampled during optimization procedures performed without symmetry constraints, although very small, are sufficient to break the local symmetry equivalence between the two NN O atoms, and (ii) the O atom which breaks the Ti–O bond also induces a shortening and strengthening of several, other Ti–O bonds formed by atoms surrounding the vacancy (see Fig. 3(D)). The remarkable, structural difference between the VOx geometries in anatase and rutile is accompanied by a parallel, remarkable difference in the electronic structure of this defect in the two compounds. In rutile, the VOx electronic structure is characterized by two spin-parallel electronic levels located at 1.0 and 1.2 eV

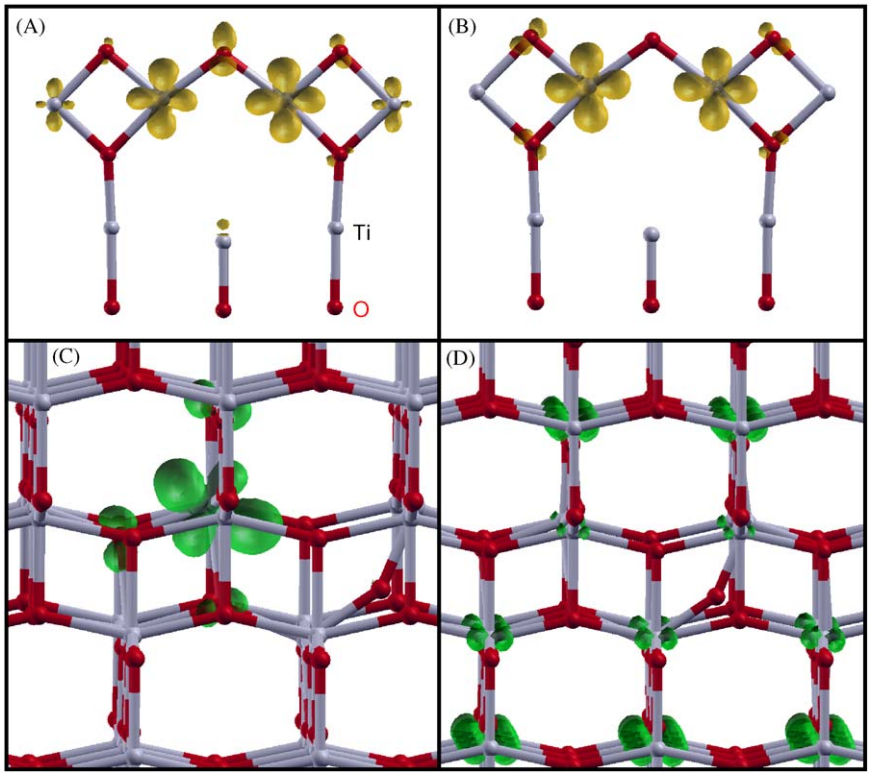

Fig. 4. Spin density distributions corresponding to the electronic levels induced by an oxygen vacancy VOx in the energy gap: (A) and (B) defect levels in rutile; (C) and (D) defect levels in anatase.

above the VBM, as shown in Fig. 2 (E). Although the estimated conduction band minimum (CBm) is at 2.0 eV from VBM against an experimental energy gap of 3.0 eV, the location of the two VOx levels suggests a deep donor behaviour of the defect, confirmed by the spin density plots of Fig. 4(A) and (B), which indicate a high localization of these levels on *d* orbitals of two Ti NN the vacancy. In the case of a VOx in anatase, instead, two spin-parallel electronic levels are found at 1.5 and 2.3 eV from VBM in correspondence with a CBm at 2.4 eV from VBM (against an experimental energy gap of 3.2 eV). These results suggest a quite different character, deep and shallow, respectively, for the two electronic levels induced by a VOx in anatase. The spin density plots corresponding to the two electronic levels, see Fig. 4(C) and (D) confirm their different characters. The lower level is indeed localized on a Ti neighbour, see the blue arrow (dashed line) in Fig. 3(D), whereas the higher level is widely delocalized on Ti atoms far from the vacancy (Fig. 4(D)). The different nature of the electronic levels induced by a VOx in anatase and rutile represents a remarkable result which can account for important differences between the properties of these two TiO_2 polymorphs, like the higher photocatalytic activity and electron mobility of anatase with respect to rutile. It has to be stressed that the LSD method gives a quite different picture: VOxs behave as shallow defects with quite similar electronic properties both in rutile and anatase.

3.3. Bulk Ti–OH defects

A H atom inserted in the rutile or anatase lattices spontaneously binds to an O atom by forming an OH-like defect (hereafter referred to as Ti–OH), as shown in Fig. 5(A) and (B) for the above two

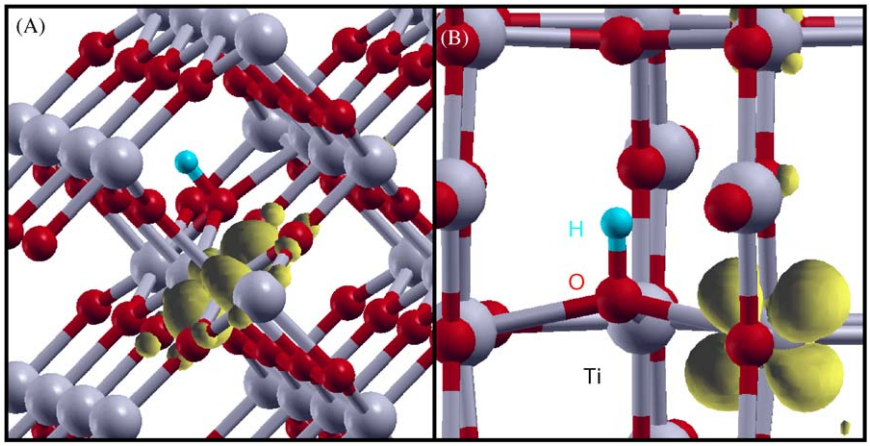

Fig. 5. Local geometry of isolated bulk Ti–OH defects and spin density plots showing the charge localization of the corresponding electronic levels: (A) Ti–OH in bulk rutile with electronic charge localized at a neighbouring Ti^{3+} atom; (B) the analogue for a Ti–OH in bulk anatase.

polymorphs, respectively. In both cases, the O–H bond has a length of about 1 Å, is perpendicular to the plane of the Ti neighbouring the O atoms, and is accompanied by small local rearrangements. In the case of rutile, the above results agree with those of a previous theoretical study [14]. The O–H bond is quite strong. In both compounds, its formation occurs indeed with an energy gain of about 2 eV with respect to the H atom in the vacuum. Moreover, two Ti–OH defects are 2.4 eV lower in energy than a H_2 molecule inserted in the lattice of either compounds. Finally, a barrier of about 0.6 eV opposes the motion of a H atom from one O atom to a neighbouring one. These results suggest a quite easy insertion as well as a high solubility of atomic H in TiO_2. Regarding the electronic properties, a bulk Ti–OH induces an electronic level located at about 1 eV and about 2 eV from the VBM in the cases of rutile and anatase, respectively, see Fig. 2. Despite their different location in the energy gap, both levels present a quite deep character as shown by the strong localization of the corresponding electronic charge, see Fig. 5. Such a localization does not involve the O–H bond. A defect electron is localized instead on a *d* orbital of a Ti atom neighbouring the Ti–OH group, that is, the H atom looses its electron by binding as a H^+ to an O atom and inducing the formation of a Ti^{3+} defect. Two Ti–OH defects do not tend to form pairs and simply induce two almost degenerate electronic levels in the energy gap. Thus, present results suggest that, in rutile, a pair of Ti–OH defects parallel the properties of a bulk VOx. Such a pair induces indeed two deep electronic levels in the energy gap as well as the formation of two Ti^{3+} defects like in the case of a VOx. Such a result implies that possible, beneficial effects produced by the VOx electronic levels in rutile, like absorption in the visible region, could be also produced by a mild insertion of atomic H in that material, like that usually performed in the case of semiconductors for electronic devices [27]. On the contrary, in anatase, a pair of Ti–OH defects does not produce the same effects of a VOx. The Ti–OH pair does not induce indeed a shallow level in the gap likely because it cannot reproduce the strong structural rearrangement accompanying the VOx formation discussed above. Notwithstanding, in the case of anatase, the presence of the H-induced level higher in energy may have positive effects on the photocatalytic properties by increasing the initial number of photoexcited carriers. As a final remark, in both polymorphs, a mild hydrogenation should permit the achievement of high concentrations of electronically active defects with minor effects on the crystal structure with respect to the introduction of VOxs, thus representing an alternative route to the conventional reduction treatments of TiO_2.

4. Conclusions

The properties of bridging hydroxyls OHb at the rutile (1 1 0) and anatase (1 0 1) surfaces as well as of oxygen vacancies and Ti–OH defects in the bulk of the same TiO_2 phases have been investigated here by using beyond-LSD, LSD + U methods. In the case of surface OHbs in rutile, a quite good agreement has been found between our results, results achieved by using hybrid functionals in a previous study and results of a recent STM study. In particular, our findings give complementary and novel information on the location of the Ti^{3+} defects which accompany the OHb defects and predict quite similar properties for the OHbs forming at the above rutile and anatase surfaces. On the contrary, a remarkable difference is found between the structural and electronic properties of bulk VOxs in rutile and anatase. In particular, the existence of a shallow level induced by bulk VOxs only in anatase is proposed here which could explain the higher electron mobility and photocatalytic activity observed for this compound with respect to rutile. Regarding the bulk Ti–OH defects, they should easily form by inserting atomic H both in rutile and anatase lattices. These defects have some similar properties in the two compounds. Moreover, in the case of rutile, the Ti–OH defects present properties quite similar to those of VOxs, thus suggesting that a mild hydrogenation could produce the same effects of an increase of VOx concentration on the material properties. In anatase, instead, Ti–OHs and VOxs have quite different properties. Notwithstanding, positive effects are expected to be produced by hydrogenation even in this material. As a general, concluding remark, it should be noted that although the results reported here regard mainly the properties of bulk VOxs and Ti–OH, these defects are expected to significantly influence even TiO_2 optical absorption. Such a process involves indeed the material surface as well as layers close to the surface where VOxs and Ti–OHs behave as in the bulk. Finally, the achieved results stress the importance of beyond-LSD methods when dealing with defects in TiO2.

Acknowledgements

The authors thank P. Giannozzi and M. Cococcioni for helpful discussion and comments and CINECA for computational resources.

References

[1] U. Diebold, Surf. Sci. Rep. 48 (2003) 53.
[2] O. Carp, C.L. Huisman, A. Reller, Prog. Solid State Chem. 32 (2004) 33.
[3] S.A. Chambers, Surf. Sci. Rep. 61 (2006) 345.
[4] M.A. Henderson, Surf. Sci. Rep. 46 (2002) 1.
[5] In Ref. [24], it has been suggested that Ti interstitials can also contribute to the n-type behaviour of rutile. A theoretical investigation of such an issue is currently in progress within our group
[6] A. Tilocca, A. Selloni, J. Phys. Chem. B 108 (2004) 4743.
[7] R. Schaub, P. Thostrup, N. Lopez, E. Lægsgaard, I. Stensgaard, J.K. Nørskov, F. Besenbacher, Phys. Rev. Lett. 87 (2001) 266104.
[8] S. Wendt, R. Schaub, J. Matthiesen, E.K. Vestergaard, E. Wahlström, M.D. Rasmussen, P. Thostrup, L.M. Molina, E. Lægsgaard, I. Stensgaard, B. Hammer, F. Besenbacher, Surf. Sci. 598 (2005) 226.
[9] O. Bikondoa, C.L. Pang, R. Ithnin, C.A. Muryn, H. Onishi, G. Thornton, Nat. Mater. 5 (2006) 189.
[10] C. Di Valentin, G. Pacchioni, A. Selloni, Phys. Rev. Lett. 97 (2006) 166803.
[11] S. Wendt, J. Matthiesen, R. Schaub, E.K. Vestergaard, E. Lægsgaard, F. Besenbacher, B. Hammer, Phys. Rev. Lett. 96 (2006) 066107.
[12] V.I. Anisimov, F. Aryasetiawan, A.I. Liechtenstein, J. Phys. Cond. Matter 9 (1997) 767.
[13] G.D. Bromiley, N. Hilairet, Miner. Mag. 69 (2005) 345.
[14] M.V. Koudriachova, S.W. de Leeuw, N.M. Harrison, Phys. Rev. B 70 (2004) 165421.
[15] S.A. Bilmes, P. Mandelbaum, F. Alvarez, N.M. Victoria, J. Phys. Chem. B 104 (2000) 9851.
[16] I. Justicia, P. Ordejón, G. Canto, J.L. Mozos, J. Fraxedas, G.A. Battiston, R. Gerbasi, A. Figueras, Adv. Mater. 14 (2002) 1399.
[17] S. Baroni, A. Dal Corso, S. de Gironcoli, P. Giannozzi, C. Cavazzoni, G. Ballabio, S. Scandolo, G. Chiarotti, P. Focher, A. Pasquarello, K. Laasonen, A. Trave, R. Car, N. Marzari, A. Kokalj, http://www.pwscf.org/.
[18] M. Cococcioni, S. de Gironcoli, Phys. Rev. B 71 (2005) 035105;
H.J. Kulik, M. Cococcioni, D.A. Scherlis, N. Marzari, Phys. Rev. Lett. 97 (2006) 103001.
[19] D. Vanderbilt, Phys. Rev. B 41 (1990) 7892.
[20] J.P. Perdew, K. Burke, M. Ernzerhof, Phys. Rev. B 77 (1996) 3865.
[21] M.M. Islam, T. Bredow, A. Gerson, Phys. Rev. B 76 (2007) 045217.
[22] R. Kurtz, R. Stockbauer, T.E. Madey, E. Romàn, J.L. De Segovia, Surf. Sci. 218 (1989) 178.
[23] M.A. Henderson, W.S. Epling, C.H.F. Peden, C.L. Perkins, J. Phys. Chem. B 107 (2003) 534.
[24] S. Wendt, P.T. Sprunger, E. Lira, G.K.H. Madsen, L. Zheshen, Ø.H. Jonas, J. Matthiesen, A. Blekinge-Rasmussen, E. Lægsgaard, B. Hammer, F. Besenbacher, Science 320 (2008) (1755).
[25] A.G. Thomas, W.L. Flavell, A.R. Kumarasinghe, A.K. Mallick, D. Tsoutsou, G.C. Smith, R. Stockbauer, S. Patel, M. Grätzel, R. Hengerer, Phys. Rev. B 67 (2003) 035110.
[26] G. Mattioli, F. Filippone, P. Alippi, A. Amore Bonapasta, Phys. Rev. B 78 (2008) 241201.
[27] J.I. Pankove, N.M. Johnson (Eds.), Semiconductors and Semimetals, Hydrogen in Semiconductors, vol. 34, Academic Press, New York, 1991.